Physical and Mechanical Properties of Wood-Based Sandwich Panels Reinforced with Basalt, Glass Fiber Fabric, and Jute Fabric

Abdurrahman Karaman [a,*] and Hikmet Yazıcı [b]

Physical and mechanical properties were investigated for wood-based sandwich panels reinforced with basalt fiber fabric (BFF), glass fiber fabric (GFF), and jute fabric (JF). The panels consist of oriented strand board (OSB) cores and beech plywood facings, with reinforcements bonded by polyurethane adhesive. Properties analyzed included screw withdrawal strength (SWS), modulus of elasticity (MOE), density (δ_{12}), and modulus of rupture (MOR). Results showed that reinforcement type significantly influenced panel performance. Jute fabric reinforcement yielded the highest stiffness (MOE of 1810 N/mm²) compared to unreinforced panels (1500 N/mm²). The BFF-reinforced panels exhibited the greatest bending strength (MOR of 62.17 N/mm²), while unreinforced panels had the lowest (53.4 N/mm²). All reinforced panels demonstrated improved SWS over unreinforced ones. Overall, reinforcing wood-based sandwich panels with jute fabric, GFF, or BFF exhibited enhanced density, bending strength, and connection strength. Reinforcement materials, including synthetic options such as glass and basalt fibers, offer lightweight, corrosion-resistant, and mechanically superior materials widely used in engineering. Natural fibers, such as jute, provide environmentally friendly reinforcement with benefits such as renewability and good insulation but face variability issues due to natural factors. The BFF composites present a promising alternative with higher tensile strength and elastic modulus than GFF, making them effective reinforcements for wood-based sandwich panels.

DOI: 10.15376/biores.21.2.3064-3080

Keywords: Reinforcement; Wood-based sandwich panel; Polyurethane adhesive; Basalt fiber fabric; Jute fabric; Physical and mechanical properties

Contact information: a: Department of Forestry, Banaz Vocational School, Uşak University, 64500 Banaz/Uşak, Turkey; b: Department of Design, Çaycuma Vocational School, Zonguldak Bülent Ecevit University, 67900 Çaycuma/Zonguldak, Turkey;
** Corresponding author: abdurrahman.karaman@usak.edu.tr*

INTRODUCTION

Moisture-curing polyurethane adhesives are widely used in fiber-reinforced composite systems due to their ability to bond reinforcements with distinct surface chemistries. The curing mechanism is based on the reaction of isocyanate groups with moisture originating from the environment or from the reinforcing fabrics, leading to the formation of a crosslinked polymer network. Consequently, the moisture content of reinforcing materials plays a critical role in curing kinetics and interfacial performance; excessive moisture, particularly in hydrophilic natural fibers, may induce foaming and interfacial defects, whereas low moisture levels in inorganic fibers can retard curing.

Moreover, the compatibility and wettability of different reinforcing fabrics by the adhesive formulation govern adhesive spreading and interfacial adhesion. Variations in surface polarity and chemical functionality among natural and inorganic fibers can significantly influence bond quality and durability (Moon *et al.* 2023).

Fiber-reinforced polymers (FRPs) are high-performance engineering materials made from continuous or polymer matrix composites reinforced with discontinuous fibers. Based on the type of reinforcement, FRP systems are typically classified as synthetic FRPs, natural fiber-reinforced polymer composites, or hybrid systems combining artificial and natural fibers (Unterweger *et al.* 2014; Xian *et al.* 2022). Common synthetic reinforcements include glass, carbon, aramid, and basalt fibers. Due to their lightweight nature, corrosion resistance, excellent fatigue resistance, high specific mechanical properties, and flexibility in structural design, FRP composites are widely used in military, marine, chemical, and civil engineering applications. In recent decades, there has been a growing interest in using FRP systems to reinforce timber elements, as these materials significantly improve mechanical strength and durability, thereby expanding the use of timber in modern construction.

In addition to synthetic fibers, natural reinforcements, such as jute, flax, sisal, and coir, have gained popularity as environmentally friendly options. Natural fiber-reinforced composites provide several advantages, including lower material costs, renewability, sound thermal and acoustic insulation, and improved energy dissipation during fracture (Gowda *et al.* 1999). Among these fibers, jute is especially favored due to its wide availability and relatively higher strength and stiffness compared to polymer matrices (Shah and Lakkad 1981). However, the mechanical properties of jute fibers vary significantly, mainly because of irregular cross-sectional shapes and sensitivity to growing conditions, geographic origin, and processing methods. These factors limit their consistency and reliability in structural load-bearing applications (Gowda *et al.* 1999).

Glass fiber-reinforced polymer (GFRP) composites are commonly produced by incorporating glass fibers into polymer matrices, such as polyester, epoxy, and vinyl ester resins, resulting in lightweight materials with high tensile strength and satisfactory chemical resistance. However, because of their inherently anisotropic properties, unidirectional GFRP composites often have limited transverse compressive strength and are more prone to stress concentrations (Li and Wang 2002). Additionally, their stiffness and tensile performance typically do not match those of carbon fiber-reinforced polymer (CFRP) systems. It is also well understood that the mechanical performance of glass fibers can be greatly affected by environmental exposure, surface modification techniques, and thermal effects (Nadir *et al.* 2016).

Recently, Basalt fiber–reinforced polymer (BFRP) composites have become a strong alternative for reinforcement materials. Compared to GFRP, BFRP offers higher tensile strength and elastic modulus, greater chemical stability, and a broader operating temperature range, all while being much more cost-effective than CFRP. Additionally, BFRP exhibits mechanical performance that surpasses that of traditional steel reinforcement while maintaining a relatively low density (Wu *et al.* 2009). These qualities have increased interest in using BFRP for strengthening and retrofitting structural systems.

Numerous experimental studies have confirmed the effectiveness of FRP reinforcements in improving the flexural behavior of timber members. Reported stiffness enhancements for GFRP-strengthened timber beams generally range from 15% to 30% (Fiorelli and Alves 2003), while increases in ultimate load-bearing capacity between 17.7%

and 77.3% have been recorded for various FRP reinforcement configurations (Yang *et al.* 2008). Borri *et al.* (2013) noted improvements in bending strength of 38.6% for low-grade and 65.8% for high-grade timber beams reinforced with flax FRP and BFRP, respectively. Similarly, Zuo *et al.* (2015) demonstrated that glulam beams strengthened with BFRP showed significant increases in ultimate bending capacity (20.9 to 111.2%), bending stiffness (18.7 to 27.6%), and ductility (23.0 to 74.3%). Comparative studies further indicated that BFRP-reinforced beams achieved approximately 20% higher ultimate bending capacity than comparable GFRP-reinforced members (Monaldo *et al.* 2019).

Karaman (2021) and Karaman and Yıldırım (2021) studied the bending moment resistance of T-shaped and L-shaped timber elements strengthened with basalt and glass woven fabrics, respectively. Kılınçarslan and Türker (2023) demonstrated that ash beams externally reinforced with BFRP in a U-shaped configuration showed significant improvements in flexural response. Türker (2024) investigated glulam beam–column connections with notched details, externally reinforced with BFRP, CFRP, and GFRP.

Screw withdrawal resistance (SWR) is a crucial mechanical property of wood-based structural materials because it directly influences the performance and dependability of mechanical fasteners. From a structural engineering standpoint, ensuring the long-term load-bearing capacity and stability of timber joints is essential (Guo *et al.* 2018). The SWR depends on various factors, including material density, screw orientation, screw size and shape, thread design, pilot hole diameter, and embedment depth. Guo *et al.* (2018) examined the SWR of traditional particleboard and bamboo-oriented strandboard and found that OSB had higher screw withdrawal strength (SWS) due to its greater density. They also observed that increasing screw diameter from 4 to 5 mm improved SWS, but further increasing it to 6 mm caused a decrease, and larger pilot holes negatively affected SWS. Perçin and Uzun (2022) investigated how heat treatment influences the SWR of laminated veneer lumber reinforced with CFRP and GFRP, concluding that higher treatment temperatures reduced SWR, while fiber reinforcement enhanced it, with no significant difference between the two fiber types. More recently, Uysal and Güntekin (2024) created predictive models to estimate the SWR of plywood-laminated MDF and particleboard panels, including both traditional and sandwich panel designs.

Although numerous studies have investigated FRP-reinforced wood composites and sandwich panel systems, most of the available literature has focused on individual reinforcement types evaluated under differing panel configurations, material combinations, and manufacturing parameters. Such variations limit the direct comparability of reported results and hinder a clear assessment of the relative effectiveness of different reinforcement systems. In particular, systematic studies directly comparing synthetic (*e.g.*, GFRP) and natural fiber–based reinforcements (*e.g.*, jute fabric) within an identical sandwich panel configuration remain scarce. Therefore, this study systematically investigates the impact of JF, GFF, and BFF reinforcements on these properties of wood-based sandwich panel specimens bonded with a room-temperature-cured polyurethane adhesive.

EXPERIMENTAL

Materials

In preparing the test specimens, both the upper and lower facings of the sandwich composites were made using 4 mm thickness beech plywood (BPWD), which was

produced from three veneer types commonly used in the furniture industry (Fig. 1a). The core layer was 9 mm thickness oriented strand board classified as OSB-2 (Fig. 1b). All wood-based materials were randomly sourced from local suppliers operating in the Uşak 1 September Industrial Area Zone. Selected physical and mechanical characteristics of these materials are presented in Table 1.

Table 1. Physical and Mechanical Properties of the Wood-based Materials Used in this Study

Physical and Mechanical Property	OSB-2 Class	4 mm BPWD
Density (kg/m^3)	670	720 to 750
Bending Strength (MOR) (N/mm^2)	22	93.9
MOE (N/mm^2)	3500	9670

Polyurethane adhesive (PUR-D4) was used for bonding and supplied by Apel Kimya Industry & Trade Co. (Turkey) (Fig. 1c). This is a single-component, moisture-curing, polyurethane-based adhesive that cures with moisture in wood and the environment. It is resistant to water, moisture, and weather conditions, D4-rated, and non-toxic. It is also suitable for bonding wood materials to each other and to various plastic materials such as metal, concrete, and polystyrene foam; it is ideal for applications requiring water resistance, such as furniture and yacht manufacturing, and boat manufacturing. The adhesive has a density of 1.11 ± 0.02 g/cm³ at 20 °C and a dynamic viscosity of 14.000 ± 3.000 mPa·s at 25 °C, as reported by the manufacturer. Under standard laboratory conditions (20 ± 2 °C and 65 ± 3% relative humidity), the initial surface setting took approximately 30 min, and the adhesive spread rate was set to 200 g/m².

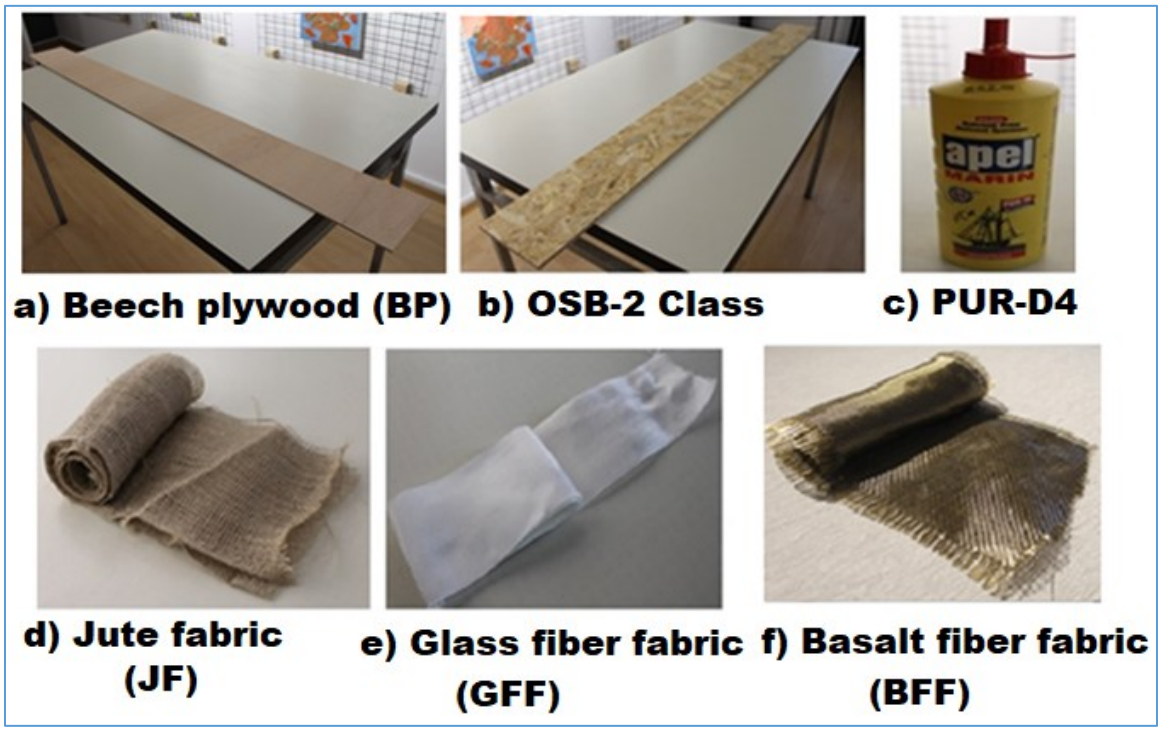

Fig. 1. Materials used in experiments

The JF for 265 g/m^2 plain materials was obtained from Polatoğlu Co. Ltd. (Turkey) (Fig. 1d). The GFF and BFF fabrics with 200 g/m^2 plain materials were sourced from Compositeshop in Turkey (Fig. 1e,f). The BFF showed a Young's modulus of 89 GPa, tensile strength of 2800 MPa, and an ultimate elongation of 3.15% (Fiore *et al.* 2011). In comparison, the corresponding values for Young's modulus, tensile strength, and fracture strain for GFF and JF were 70 and 26.5 GPa, 2000 to 3500 and 393 to 773 MPa, and 0.9% and 1.8%, respectively (Pai and Jagtap 2015).

Preparation and Construction of Specimens

The OSB-2 panels and 4 mm thickness BPWD sheets were precisely cut into 31 specimens per panel using a computer numerical controlled (CNC) system, with final dimensions of 165 × 1800 ± 1 mm (Fig. 2a).

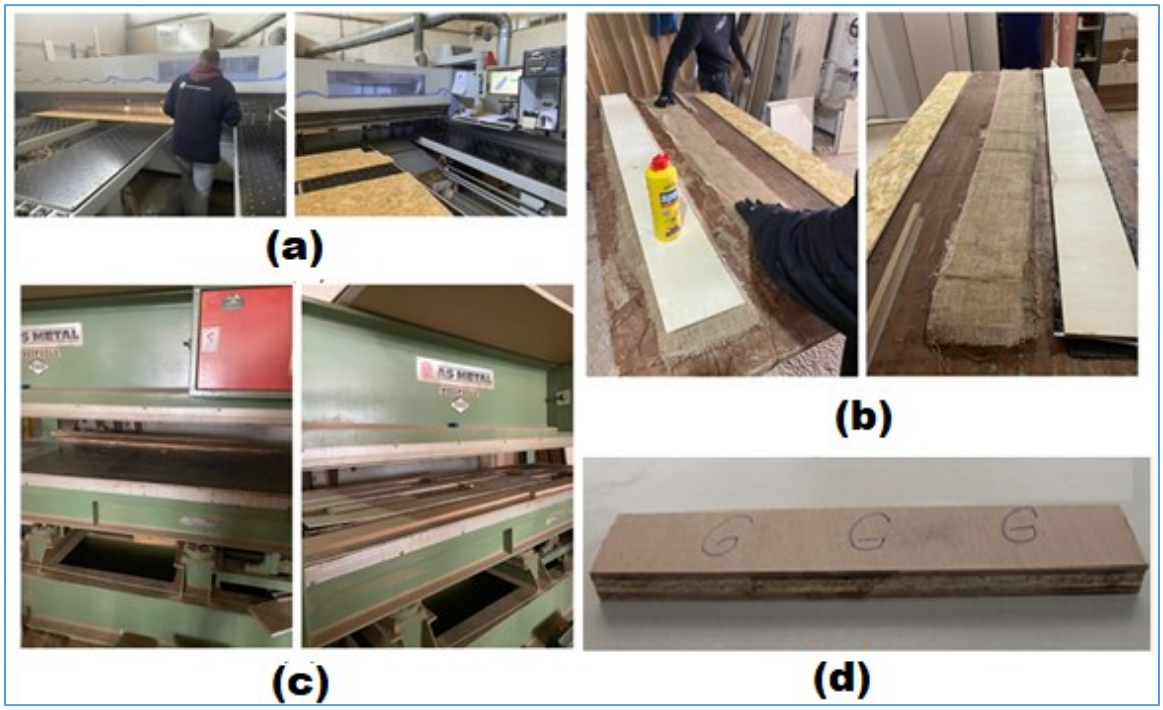

Fig. 2. The production process of test samples

Two reinforcement layers were applied at the interfaces between the MDF faces and the OSB core to achieve symmetric reinforcement and balanced stress distribution under mechanical loading. This configuration was selected to enhance interfacial stress transfer while avoiding excessive increases in panel thickness and density. Alternative configurations were considered but not included in this study to maintain a controlled and comparable panel design. The adhesive was applied uniformly to the bonding surfaces at an average spread rate of approximately 200 g/m² (Fig 2b). Basalt fiber fabric, glass fiber fabric, or jute fabric was placed as an interlayer reinforcement between the OSB core and the plywood face layers. Panel fabrication was carried out using a hydraulic press under cold-pressing conditions applying a constant pressure of approximately 1.5 N/mm² at at 25 °C for a curing period of 3 h (Fig. 2c). The pressing process is shown in Fig. 2d. After pressing, the panels were removed from the press and conditioned under laboratory

ambient conditions until equilibrium moisture content was reached prior to specimen preparation and mechanical testing. The different sandwich panel configurations produced in this study are summarized in Table 2.

Table 2. Combinations of Wood-based Sandwich Panels Manufactured

Groups	Code	Face Layer	Reinforcement Types	Core Layer	Bottom Layer
E	BP-B-O-B-BP	BP (BPWD)	B (BFF)	O (OSB-2 class)	BP (BPWD)
F	BP-J-O-J-BP	BP (BPWD)	J (Jute fabrics)	O (OSB-2 class)	BP (BPWD)
G	BP-G-O-G-BP	BP (BPWD)	G (GFF)	O (OSB-2 class)	BP (BPWD)
H	BP-O-BP	BP (BPWD)	Unreinforced	O (OSB-2 class)	BP (BPWD)

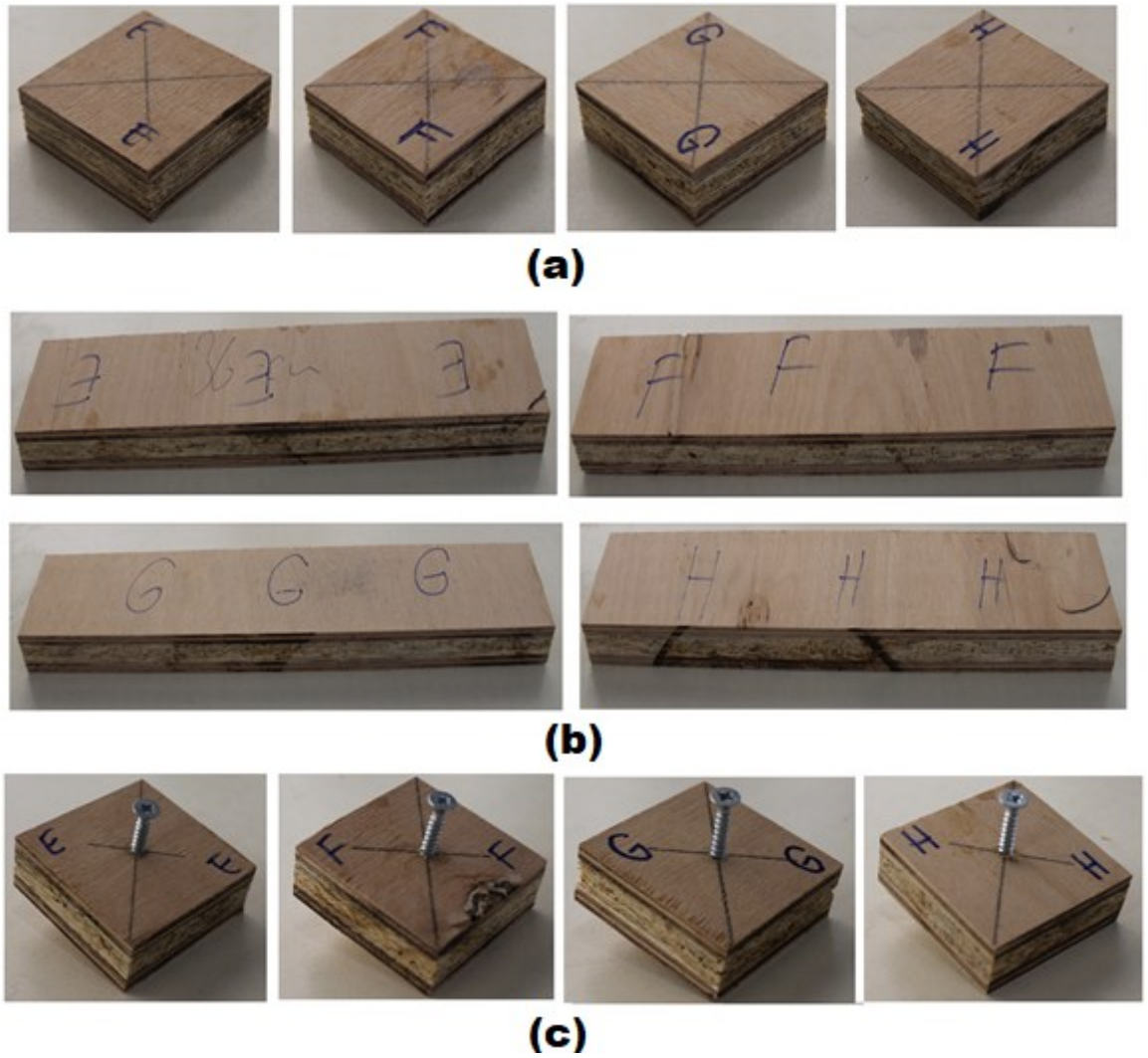

Fig. 3. The configuration of test samples: a) Test samples of air-dry density, b) Test samples of modulus of elasticity in bending and of bending strength, c) Test samples of screw withdrawal resistance

The determination of the MOR, MOE, δ_{12}, and SWR was conducted following TS EN 310 (1999), TS EN 323 (1999), and TS EN 13446 (2002), respectively. For each mechanical property, ten specimens were prepared per experimental group to ensure statistical validity. Before testing, all manufactured panels were conditioned for three weeks in a climate-controlled chamber set at 20 ± 2 °C and 65 ± 5% relative humidity.

After conditioning, test specimens were cut from the panels following relevant standards. Samples for density and SWS measurements were cut to nominal dimensions of 50 × 50 mm (Fig. 3a), while bending test specimens for MOR and MOE were prepared with dimensions of 50 × 410 mm (Fig. 3b).

For screw withdrawal tests, pilot holes corresponding to 80% of the nominal screw diameter were drilled perpendicular to the panel surface. The screws were then inserted so that the full length of the threaded part passed through the specimen, with the screw tip protruding beyond the opposite face, as shown in Fig. 3c.

Methods of Loading and Testing

Density

The air-dry density of the test samples was determined in accordance with the TS EN 323 (1999) standard. The δ_{12} was determined using Eq. 1,

$$\delta_{12} = \frac{M_{12}}{V_{12}} \quad (1)$$

where δ_{12} is the air-dry density (kg/m³), M_{12} represents the air-dry mass (kg), and V_{12} denotes the specimen volume (m³).

Bending Strength (MOR) and MOE

Bending test specimens were prepared with dimensions of 410 × 50 × 18 mm^3. Ten specimens were tested for each experimental group. A three-point bending setup was used (Fig. 4), with the support span (L_1) set to 20 times the specimen thickness and the total specimen length (L_2) defined as L_1 + 50 mm. Mechanical tests were conducted using a 10 kN electromechanical universal testing machine at Kütahya Dumlupınar University. The loading rate was maintained at 2 mm/min

The MOR and MOE were calculated using Eqs. 2 and 3, respectively,

$$MOR = \frac{F_{max} \times L_1}{2 \times b \times h^2} \quad (2)$$

where F_{max} represents the maximum load (N), L_1 is the length of test samples (mm), b is the width of test samples (mm), and h is the thickness of test samples (mm).

$$MOE = \frac{\Delta F \times {L_1}^3}{4 \times b \times h^3 \times \Delta f} \quad (3)$$

In Eq. 3, ΔF represents the load difference within the proportional limit (N); L_1 is the length of test samples (mm), b is the width of test samples (mm), h is the thickness of test samples (mm), and Δf corresponds to the associated deflection difference (mm).

Screw withdrawal strength

The SWS tests were conducted according to the TS EN 13446 (2002) standards using a SHIMADZU universal testing machine. Withdrawal forces were applied parallel

to the screw axis at a steady displacement rate of 2 mm/min until failure (Fig. 5). The SWS values were calculated using Eq. 4.

$$\sigma_{SWS} = \frac{F_{max}}{d \times l_p} \quad (4)$$

where F_{max} is the ultimate withdrawal load (N), d is the screw diameter (mm), and l_p is the penetration depth of the screw (mm).

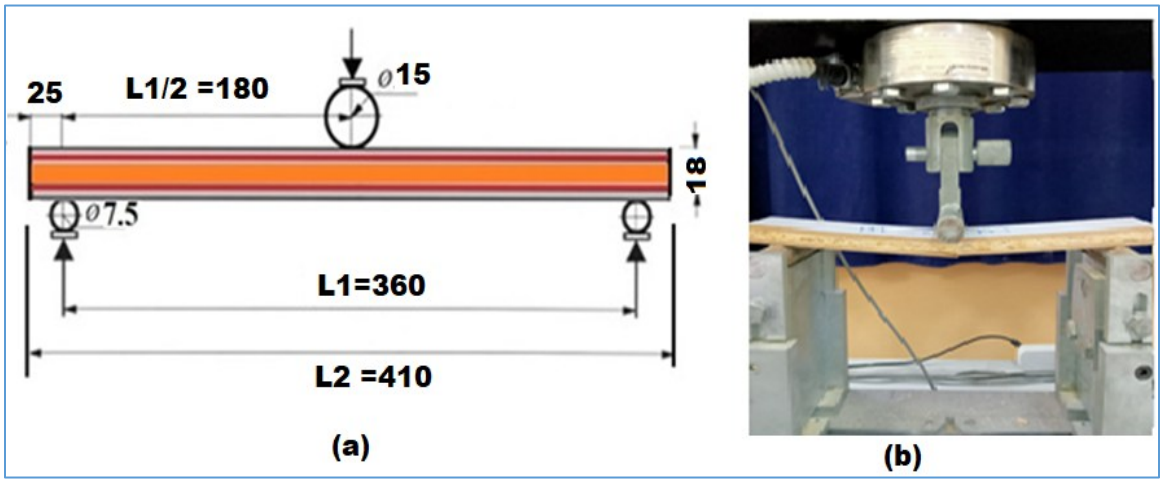

Fig. 4. Three-point bending test set-up for test samples: (a) the static system (in mm), (b) testing

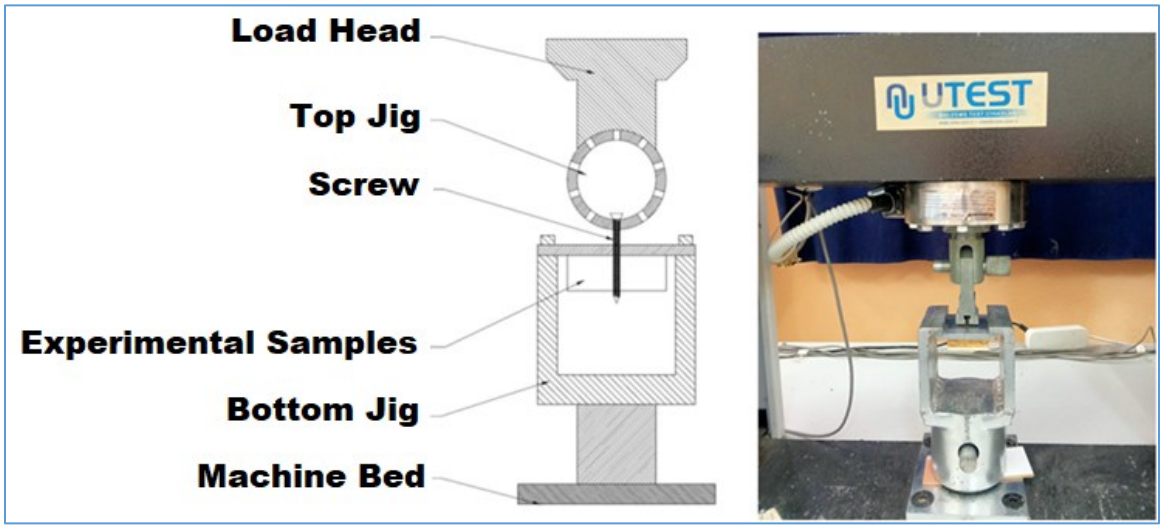

Fig. 5. Test configuration for screw withdrawal strength from the face

Statistical Analysis

Statistical evaluations were performed using Minitab® 18 software (State College, PA, USA). Analysis of variance (ANOVA) was applied, and mean comparisons were carried out using the Duncan multiple range test at a significance level of $p < 0.05$. Prior to Duncan's multiple range test, the suitability of ANOVA assumptions was assessed through residual analysis.

RESULTS AND DISCUSSION

According to the experimental results, the statistical values for specific physical and mechanical properties of the samples are shown in Table 3.

Table 3. Statistical Values of Some Physical and Mechanical Properties

Groups	Values	δ_{12} (kg/m^3)	MOR (N/mm^2)	MOE (N/mm^2)	SWS (N/mm^2)
E	$\bar{x}$	730	59.53	1504	27.23
	SD	10.92	3.33	168	4.02
	COV (%)	1.50	5.66	11.17	14.76
	Min.	715	55.86	1221	22.98
	Max.	750	67.06	1714	34.75
	N	10	10	10	10
F	$\bar{x}$	708	55.20	1818	26.82
	SD	6.35	4.96	117	3.13
	COV (%)	0.90	8.98	6.44	11.67
	Min.	700	47.71	1575	22.71
	Max.	715	63.08	1952	32.10
	N	10	10	10	10
G	$\bar{x}$	740	62.17	1710	28.75
	SD	12.69	3.00	147	4.25
	COV (%)	1.71	4.83	8.60	14.78
	Min.	765	58.29	1452	22.89
	Max.	728	67.07	1901	36.88
	N	10	10	10	10
H	$\bar{x}$	687	53.47	1576	24.36
	SD	8.18	3.81	130	4.04
	COV (%)	1.19	7.13	8.23	16.58
	Min.	675	57.74	1416	15.15
	Max.	700	60.51	1754	28.34
	N	10	10	10	10

$\bar{x}$: Average values, SD: Standard deviation, COV (%): Coefficient of variation, N: Number of samples. E: basalt fiber fabric reinforced configuration, F: jute fabric reinforced configuration, G: glass fiber fabric reinforced configuration, and H: unreinforced configuration

The comparison among the E, F, G, and H groups was determined by ANOVA (Table 4). According to the analysis, differences in δ_{12}, MOR, MOE, and SWS were statistically significant at the 0.05 level.

According to the ANOVA results in Table 4, the differences between the groups were statistically significant in terms of the δ_{12}, MOR, and MOE (P<0.05), while the differences between the groups in terms of SWS were statistically insignificant at the level of 0.05. The results of the Duncan test, which was conducted to determine which groups differed significantly, are given in Table 5.

Table 4. ANOVA Results

	Source	SO	DF	MS	F Value	P < 0.05
δ_{12} (kg/m³)	Between Groups	17286.875	3	5762.292	59.482	0.000
	Within Groups	3487.500	36	96.875		
	Total	20774.375	39			
	Source	**SO**	**DF**	**MS**	**F Value**	**P < 0.05**
MOR (N/mm²)	Between Groups	484.309	3	161.436	10.896	0.000
	Within Groups	533.401	36	14.817		
	Total	1017.709	39			
	Source	**SO**	**DF**	**MS**	**F Value**	**P < 0.05**
MOE (N/mm²)	Between Groups	586180.100	3	195393.367	9.702	0.000
	Within Groups	725001.800	36	20138.939		
	Total	1311181.900	39			
	Source	**SO**	**DF**	**MS**	**F Value**	**P < 0.05**
SWS (N/mm²)	Between Groups	99.250	3	33.083	2.194	0.106
	Within Groups	542.801	36	15.078		
	Total	642.051	39			

SO: Sum of Squares, DF: Degrees of freedom, MS: Mean Squares

Table 5. Duncan Test Results

Groups	Physical and Mechanical Properties							
	δ_{12} (kg/m³)		MOR (N/mm²)		MOE (N/mm²)		SWS (N/mm²)	
	x̄	HG	X	HG	x̄	HG	x̄	HG
E	730	A	59.53	AB	1504	C	27.23	A
F	708	B	55.20	BC	1810	A	26.82	A
G	740	A	62.17	A	1710	AB	28.75	A
H	687	C	53.35	C	1576	BC	24.36	A

x̄: Average values, HG: Homogeneity groups

As summarized in Table 5, notable variations were observed in the δ_{12} of the tested sandwich panel groups. Compared to the unreinforced configuration (Group H), all panels with BFF, GFF, or jute fabric showed increased density values. This trend mainly results from improved adhesive penetration and distribution within the panel structure caused by the reinforcement layers. Among all configurations, Group G achieved the highest δ_{12} at 740 kg/m³, while Group H had the lowest at 687 kg/m³. Intermediate density values of 708 and 730 kg/m³ were noted for Groups F and E, respectively. These results clearly demonstrate that incorporating fiber-based reinforcements during fabrication helps create a denser sandwich panel structure.

The bending strength results further emphasized the beneficial effect of reinforcement materials. The highest MOR was recorded with Group G specimens, reaching 62.2 N/mm², while the unreinforced Group H panels had the lowest MOR at 53.4 N/mm². Groups E and F showed intermediate MOR values of 59.5 and 55.2 N/mm², respectively. The increase in bending strength for reinforced panels can be attributed to the load-sharing ability and the superior tensile properties of the BFF, GFF, and jute fabrics layers embedded within the sandwich structure.

Regarding stiffness, the MOE results showed a wider range among the tested groups. The lowest MOE value of 1500 N/mm² was observed in Group E, while Group F exhibited the highest stiffness at 1810 N/mm². The other configurations had MOE values within this range, with 1580 N/mm² for Group H and 1710 N/mm² for Group G. These differences indicate that both reinforcement type and interlayer configuration significantly influence the elastic response of the WBSP.

In this study, the modulus of elasticity (MOE) was obtained from three-point bending tests using conventional bending-based expressions. For sandwich-type layered panels, the measured mid-span deflection can comprise both bending and transverse shear components, especially when the core or interlayer exhibits relatively low shear rigidity. Accordingly, within a Timoshenko-type framework, the reported MOE should be regarded as an apparent modulus that incorporates the combined influence of bending stiffness and shear compliance rather than a purely bending-related property. Since all specimens were tested under identical geometric conditions, span-to-thickness ratios, and loading protocols, the relative contribution of transverse shear deformation is expected to be similar for all configurations, thereby maintaining the reliability of comparative evaluations among the different reinforcement variants.

The SWS analysis showed consistent improvements across all reinforced panels compared to the unreinforced reference. Group G recorded the highest average SWS at 28.75 N/mm², with a standard deviation of 4.05 N/mm². Next, was Group F, with an average SWS of 27.23 N/mm² and a standard deviation of 4.02 N/mm². Group E achieved lower but still improved SWS values of 26.82 N/mm², while Group H had the lowest average at 24.07 N/mm².

According to the statistical analysis presented in Table 5, no significant differences were detected among the experimental groups in terms of screw withdrawal strength, as all groups were classified within the same homogeneity group (HG = A). Consequently, the higher mean SWS values observed in some reinforced panels represent numerical tendencies rather than statistically confirmed improvements.

Previous research consistently indicates that higher material density generally results in increased screw withdrawal strength (Bal *et al.* 2017; Jivkov *et al.* 2017). Conversely, excessively high elastic stiffness may decrease effective thread engagement, creating an inverse relationship between MOE and SWS in some wood-based materials (Yunus *et al.* 2019). Additionally, increases in density caused by reinforcement have been identified as an important factor in enhancing screw withdrawal performance (Perçin and Uzun 2022).

The positive impacts of fiber-reinforced polymer systems on the flexural performance of wood-based composites are well established. For example, Ding (2008) found that basalt fiber reinforcement increased bending strength by up to 200% in structural plywood. Other sandwich configurations, such as corrugated bamboo-based systems, have also shown excellent mechanical performance, with MOR and MOE values reaching as

high as 38.5 and 5210 N/mm², respectively (Yang and Fei 2012; Smardzewski *et al.* 2022). Similarly, sandwich panels with GFRP skins and uniform balsa cores demonstrated flexural strengths ranging from 29.9 to 34.1 N/mm² (Osei-Antwi *et al.* 2014).

Further improvements in bending performance have been achieved through optimized resin selection and reinforcement layout. Moradpour *et al.* (2018) demonstrated that combining GFRP reinforcement with pMDI resin increased MOR and MOE 123% and 114%, respectively, compared to unreinforced panels. Generally, the stiffness of wood-based composites is primarily determined by the elastic properties of their constituent materials. Because the elastic modulus of GFRP is roughly 10 times that of poplar wood, the observed increase in stiffness can be directly attributed to the reinforcement layers.

Additional studies have highlighted the significance of reinforcement geometry. Bakalarz and Kossakowski (2019) reported increases of approximately 20% in bending strength for bottom-face GFRP reinforcement and 22% for U-shaped configurations. Similarly, GFRP-faced honeycomb sandwich panels exhibited flexural performance that depends heavily on core composition, with maximum bending stresses recorded as 13.3, 42.0, and 107.14 N/mm² for MDF, wheat straw, and plywood cores, respectively (Hussain *et al.* 2019).

Advanced sandwich architectures with innovative core designs have further improved structural efficiency. Panels with auxetic wooden cores achieved MOE and MOR values of 3300 N/mm² and 26.6 N/mm², respectively, while keeping densities below 400 kg/m³ (Smardzewski 2019). Similarly, multilayer wood-based sandwich panels bonded with polyurethane adhesives reached very high MOE and MOR values of up to 8880 and 92.9 N/mm², respectively (Gozdecki and Kociszewski 2021). More recently, Cordier and Mai (2025) reported MOR increases of up to 25% in the parallel direction and up to 49% in the perpendicular direction for plywood reinforced with acrylate-coated basalt fiber grids after normalization for density.

Screw withdrawal performance is affected by several factors, including wood species, density, fiber orientation, moisture content, screw design, surface treatment, and embedment depth (Kılıç *et al.* 2006). Perçin and Uzun (2022) demonstrated that adding glass and carbon fiber reinforcement significantly boosted the SWS of heat-treated Scots pine, with improvements of up to 49%, depending on the loading direction. Kaya and İmirzi (2023) reported that wood-based composite panels with corrugated core geometries had screw holding resistances ranging from 8.92 to 15.36 N/mm², depending on core shape and surface material.

Predictive modeling studies have further confirmed the strong connection between panel density and screw withdrawal resistance in plywood-laminated MDF, particleboard, and sandwich panel systems. The highest predicted SWS value of 12.5 N/mm² was obtained for plywood–MDF sandwich panels, while the differences between experimental and predicted values ranged from 0.20% to 24.9% (Uysal and Güntekin 2024).

The differences observed in stiffness and strength among the reinforced sandwich panels can be attributed to the distinct mechanical properties and structural characteristics of the reinforcement materials. High-stiffness reinforcements such as GFRP promote more efficient stress transfer across the face–core interface, leading to improved load sharing between the MDF faces and the OSB core. In contrast, natural fiber–based reinforcements, such as jute fabric, exhibit lower elastic modulus and higher compliance, which may result in reduced stress transfer efficiency but contribute to lower density and improved deformability. The placement of the reinforcement layer at the interface between the face

and core plays a critical role in limiting interlaminar shear deformation and delaying damage initiation, thereby influencing the overall mechanical response of the sandwich panel.

For future research on wood-based sandwich panel systems, several key areas are recommended. These include exploring alternative panel combinations, such as plywood and particleboard, evaluating epoxy and polyvinyl acetate (PVAc) adhesives as bonding agents, investigating advanced reinforcement textiles including Kevlar, cotton, and aramid fibers, and thoroughly assessing the sound absorption and related mechanical properties of panels made with these materials.

CONCLUSIONS

The current study systematically examined the modulus of elasticity (MOE), modulus of rupture (MOR), density (δ_{12}), and screw withdrawal strength (SWS) of wood-based sandwich panels, both unreinforced and reinforced with basalt fiber fabric (BFF), jute fabric (JF), and glass fiber fabric (GFF), using a polyurethane (PUR-D4) adhesive cured under ambient conditions.

1. The experimental results indicated that the type of reinforcing fiber had a statistically significant impact on the MOE, MOR, δ_{12}, and SWS of the sandwich panel specimens.
2. With respect to screw withdrawal strength, although variations in mean values were observed among the reinforcement configurations, no statistically significant differences were identified. Therefore, the observed differences should be interpreted as numerical trends rather than evidence of the superiority of a specific reinforcement system.
3. Regardless of the reinforcement material, specimens with BFF, GFF, or JF showed higher δ_{12}, MOR, MOE, and SWS values than the unreinforced reference panels.
4. The highest density, MOR, MOE, and SWS values were obtained in the experimental samples reinforced with glass fiber fabric.
5. In contrast, panels reinforced with jute fabric showed greater bending stiffness, as indicated by higher MOE values.
6. Overall, the findings confirm that reinforcing wood-based sandwich panels with JF, BFF, and GFR significantly improved their density, flexural performance, and connection-related mechanical properties compared to unreinforced configurations.
7. Overall, the experimental results indicate that the incorporation of reinforcement layers influences the mechanical response of wood-based sandwich panels, although some effects are expressed as numerical trends rather than statistically significant differences. Beyond the comparison of individual reinforcement types, this study provides general insights into the role of interfacial reinforcement in governing stress transfer and stiffness development in sandwich panel systems. The findings demonstrate that reinforcement effectiveness depends not only on material type but also on its placement and interaction with the face–core interface, offering design-

oriented guidance applicable to a wide range of reinforced wood-based sandwich structures.

ACKNOWLEDGMENTS

The author declares that there are no funds to acknowledge and no conflict of interest.

REFERENCES CITED

Bakalarz, M., and Kossakowski, P. (2019). "The flexural capacity of laminated veneer lumber beams strengthened with AFRP and GFRP sheets," *Technical Transactions* 116, 85-96. https://doi.org/10.4467/2353737XCT.19.023.10159

Bal, B. C., Akcakaya, E., and Gundes, Z. (2017). "Screw-holding capacity of melamine-faced fiberboard and particleboard used in furniture production," *Mugla Journal of Science and Technology* 4, 49-52.

Borri, A., Corradi, M., and Speranzini, E. (2013). "Reinforcement of wood with natural fibers," *Composites Part B: Engineering* 53, 1-8. https://doi.org/10.1016/j.compositesb.2013.04.039

Cordier, M., and Mai, C. (2025). "Basalt grid reinforcement of lightweight plywood," *European Journal of Wood and Wood Products* 83(1), article 45. https://doi.org/10.1007/s00107-024-02196-7

Fossetti, M., Minafò, G., and Papia, M. (2015). "Flexural behavior of glulam timber beams reinforced with FRP cords," *Construction and Building Materials* 95, 54-64. https://doi.org/10.1016/j.conbuildmat.2015.07.116

Fiorelli, J., and Alves, S. M. (2003). "Analysis of the strength and stiffness of timber beams reinforced with carbon fiber and glass fiber," *Materials Research* 6(2), 193-202. https://doi.org/10.1590/S1516-14392003000200016

Fiore, V., Di Bella, G., and Valenza, A. (2011). "Glass–basalt/epoxy hybrid composites for marine applications," *Materials & Design* 32(4), 2091-2099. https://doi.org/10.1016/j.matdes.2010.11.043

Gowda, T. M., Naidu, A. C. B., and Chhaya, R. (1999). "Some mechanical properties of untreated jute fabric-reinforced polyester composites," *Composites Part A: Applied Science and Manufacturing* 30(3), 277-284. https://doi.org/10.1016/S1359-835X(98)00157-2

Gozdecki, C., and Kociszewski, M. (2021). "The properties of sandwich panels made of standard wood-based panels," *Annals of Warsaw University of Life Sciences SGGW Forestry and Wood Technology* 114, 125-130. https://doi.org/10.5604/01.3001.0015.2411

Hussain, M., Abbas, N., Zahra, N., Sajjad, U., and Awan, M. B. (2019). "Investigating the performance of GFRP/wood-based honeycomb sandwich panels for sustainable prefab building construction," *SN Applied Sciences* 1, article 875. https://doi.org/10.1007/s42452-019-0932-3

Jivkov, V., Kyuchukov, B., Simeonova, R., and Marinova, A. (2017). "Withdrawal capacity of screws and confirmat into different wood-based panels," in: *Proceedings*

of the XXVIIIth International Conference on Rresearch for Furniture Industry, Poznan, Poland, pp. 68-82.

Karaman, A. (2021). "Bending moment resistance of T-type joints reinforced with basalt and glass woven fabric materials," *Maderas. Ciencia y Tecnología* 23, article 444. https://doi.org/10.4067/s0718-221x2021000100444

Karaman, A., and Yildirim, M. N. (2021). "Effects of wood species of the dowels and fiber woven fabric types on bending moment resistance of L-shaped joints," *Wood Industry and Engineering* 3(2), 12-22.

Kaya, M., and Imirzi, H. O. (2023). "Determination of screw holding resistance of wood-based composite panels with different geometric corrugated core," *Furniture and Wooden Material Research Journal* 6(1), 123-133. https://doi.org/10.33725/mamad.1264176

Kılıç, M., Burdurlu, E., Usta, İ., Berker, U. Ö., and Oduncu, P. (2006). "Comparative analysis of the nail and screw withdrawal resistances of fir (*Abies* Mill.), cherry (*Prunus avium* L.), walnut (*Juglans regia* L.) and oak (*Quercus* L.) wood," *Duzce University Journal of Forestry* 2(2), 61-75.

Kilinçarslan, S., and Türker, Y. S. (2023). "Strengthening of the solid beam with fiber-reinforced polymers," *Turkish Journal of Engineering* 7(3), 166-171. https://doi.org/10.31127/tuje.1026075

Li, V. C., and Wang, S. (2002). "Flexural behaviors of glass fiber-reinforced polymer (GFRP) reinforced engineered cementitious composite beams," *Materials Journal* 99(1), 11-21.

Lu, W., Ling, Z., Geng, Q., Liu, W., Yang, H., and Yue, K. (2015). "Study on flexural behavior of glulam beams reinforced by near surface mounted (NSM) CFRP laminates," *Construction and Building Materials* 91, 23-31. https://doi.org/10.1016/j.conbuildmat.2015.04.050

Meekum, U., and Mingmongkol, Y. (2011). "Experimental design on laminated veneer lumber fiber reinforced composite: Processing parameters and its durability," in: *16th International Conference on Composite Structures-ICCS 16*, Porto, Portugal, pp. 1029-1038.

Micelli, F., Scialpi, V., and La Tegola, A. (2005). "Flexural reinforcement of glulam timber beams and joints with carbon fiber-reinforced polymer rods," *Journal of Composites for Construction* 9(4), 337-347. https://doi.org/10.1061/(ASCE)1090-0268(2005)9:4(337)

Monaldoa, E., Nerillia F., and Vairo, G. (2019). "Basalt-based fiber-reinforced materials and structural applications in civil engineering," *Composite Structures* 214, 246-263. https://doi.org/10.1016/j.compstruct.2019.02.002

Moradpour, P., Pirayesh, H., Gerami, M., and Jouybari, I. R. (2018). "Laminated strand lumber (LSL) reinforced by GFRP; mechanical and physical properties," *Construction and Building Materials* 158, 236-242. https://doi.org/10.1016/j.conbuildmat.2017.09.172

Moon, H., Park, J. E., Cho, W., Jeon, J., and Wie, J. J. (2023). "Curing kinetics and structure-property relationship of moisture-cured one-component polyurethane adhesives," *European Polymer Journal* 201, article 112579. https://doi.org/10.1016/j.eurpolymj.2023.112579

Nadir, Y., Nagarajan, P., and Ameen, M. (2016). "Flexural stiffness and strength enhancement of horizontally glued laminated wood beams with GFRP and CFRP

composite sheets," *Construction and Building Materials* 112, 547-555. https://doi.org/10.1016/j.conbuildmat.2016.02.133

Osei-Antwi, M., de Castro, J., Vassilopoulos, A. P., and Keller, T. (2014). "Fracture in complex balsa cores of fiber-reinforced polymer sandwich structures," *Construction and Building Materials* 71, 194-201. https://doi.org/10.1016/j.conbuildmat.2014.08.029

Pai, A. R., and Jagtap, R. N. (2015). "Surface morphology & mechanical properties of some unique natural fiber reinforced polymer composites-a review," *Journal of. Materials and Environmental Science* 6(4), 902-917.

Perçin, O., and Uzun, O. (2022). "Screw withdrawal strength of heat-treated and laminated veneer lumber reinforced with carbon and glass fibers," *BioResources* 17(2), 2486-2500. https://doi.org/10.15376/biores.17.2.2486-2500

Shah, A. N., and Lakkad, S. C. (1981). "Mechanical properties of jute-reinforced plastics," *Fibre Science and Technology* 15(1), 41-46.

Smardzewski, J. (2019). "Experimental and numerical analysis of wooden sandwich panels with an auxetic core and oval cells," *Materials & Design* 183, article 108159. https://doi.org/10.1016/j.matdes.2019.108159

Smardzewski, J., Krzyzaniak, Ł., Wojciechowski, K. W., Pelínski, K., Tretiakov, K. V., and Narojczyk, J. W. (2022). "Bending performance and failure behavior of wooden sandwich panels with corrugated cores," *Physica Status Solidi (B): Basic Research* 259(12), article 2200423. https://doi.org/10.1002/pssb.202200423

TS EN 323 (1999). "Wood-based panels – Determination of density," Turkish Standards Institute, Ankara, Turkey.

TS EN 326-1 (1999). "Wood-based panels – Sampling, cutting and inspection – Part 1: Sampling and cutting of test pieces and expression of test results," Turkish Standards Institute, Ankara, Turkey.

TS EN 13446 (2002). "Wood-based panels – Determination of withdrawal capacity of fasteners," Turkish Standards Institute, Ankara, Turkey.

Turker, Y. S. (2024). "Experimental Investigation of rotational behavior of glulam column-beam connection reinforced with carbon, glass, basalt and aramid FRP fabric," *Drvna Industrija* 75(2), 259-270. https://doi.org/10.5552/drvind.2024.0162

Unterweger, C., Brüggemann, O., and Fürst, C. (2014). "Synthetic fibers and thermoplastic short-fiber-reinforced polymers: Properties and characterization," *Polymer Composites* 35(2), 226-236. https://doi.org/10.1002/pc.22654

Uysal, B., and Güntekin, E. (2024). "Prediction of screw withdrawal resistance for plywood laminated panels and sandwich panels," *Turkish Journal of Forestry* 25(1), 81-88. http://dx.doi.org/10.18182/tjf.1375273

Xian, G., Guo, R., and Li, C. (2022). "Combined effects of sustained bending loading, water immersion and fiber hybrid mode on the mechanical properties of carbon/glass fiber reinforced polymer composite," *Composite Structures* 281, article ID 115060. https://doi.org/10.1016/j.compstruct.2021.115060

Wu, Z., Wang, X., and Wu, G. (2009, July). "Basalt FRP composite as reinforcements in infrastructure," in: *Proceedings of the 17th Annual International Conference on Composites/Nano Engineering (ICCE-17)*, New Orleans, LA, USA, pp. 21-24.

Yang, H., and Liu, W. (2007). "Study on flexural behavior of FRP reinforced glulam beams," *Journal of Building Structures* 28(1), 64-71.

Yang, H., Liu, W., and Xiong, J. (2008). "Experimental study on flexural behavior of FRP reinforced wood beams," *Materials and Structures* 41(1), 161-170. https://doi.org/10.1617/s11527-007-9234-7

Yang, F., and Fei, B.(2012). "The research on bamboo-wood corrugated sandwich panel," in: *Proceedings of the 55th International Convention of Society of Wood Science and Technology*, Beijing, China, pp.1-8.

Yunus, N. Y. M., Amali, N. W. A., Tamat, N. S. M., and Rahman, W. M. N. W. A. (2019). "Flexural influence on screw withdrawal behavior of selected commercial particleboard," *International Journal of Advanced Engineering and Technology* 9, 5948-5951. https://doi.org/10.35940/ijeat.A3033.109119

Zuo, H., Bu, D., Guo, N., and He, D. (2015). "Effect of basalt fiber composite on flexural behavior of glulam beams," *Journal of Northeast Forestry University* 43(4), 91-95. https://doi.org/10.13759/j.cnki.dlxb.20150116.0

Article submitted: December 24, 2025; Peer review completed: January 31, 2026; Revised version received and accepted: February 1, 2026; Published: February 11, 2026.
DOI: 10.15376/biores.21.2.3064-3080